Characterization and Nitrile Group Hydrogenation Study of Supported and Unsupported Ru–Co Catalyst

Haruhiko Kusaka, Yoshinori Hara, Masamichi Onuki, Toshio Akai,* and Masami Okuda*

*Chemical Laboratory and *Analytical Laboratory, Mitsubishi Chemical Corporation, Yokohama Research Center 1000, Kamoshida-cho, Aoba-ku, Yokohama 227, Japan*

Characterization studies of a mixed Ru–Co catalyst unsupported and supported on SiO_2 were performed. We also examined the effect of the catalyst on hydrogenation of nitrile compounds. TPR shows that Co(II) in an unsupported $Ru(OH)x/Co(OH)y$ precursor is easily reduced at around 473–573 K, whereas the hydrogen reduction of Co(II) in the $Ru(OH)x–Co(OH)y/SiO_2$ did not occur even at 873 K. X-ray adsorption fine structure measurements indicated that both metals of the unsupported Ru/Co catalyst are reduced to their respective metallic state, and it is thought that Co^0–Ru^0 alloy is formed. However, Ru and Co exist as Ru^0 metal and Co oxide, respectively, in the case of a SiO_2 supported catalyst. An unsupported Ru–Co catalyst shows higher activity for the hydrogenation of nitrile group and reductive amination of C=O group of isophoronenitrile and the hydrogenation of nitrile groups of adiponitrile, succinonitrile, and dicyanobenzene than the SiO_2 supported catalyst does. It is suggested that this high performance of the unsupported catalyst is based on the formation of Ru^0–Co^0 alloy. © 1996 Academic Press, Inc.

INTRODUCTION

Both Ru and Co are realized as very important metals in the field of hydrogenation catalysts with some reports of synergistic effects of Ru–Co. In Fischer–Tropsch synthesis, in general, the incorporation of a small amount of Ru in supported Co catalysts is said to improve the activity and C_5^+ selectivity (1–7).

E. Iglesia *et al.* reported that deactivated Ru–Co catalysts could be regenerated by hydrogenation treatment, whereas a monometallic Co catalyst could not. The cause of this phenomenon is thought to be that Ru enhances the catalytic hydrogenolysis of carboneous residuers and diminishes the surface oxygen species under H_2 atmosphere (7).

Ichikawa *et al.* reported that the activity and selectivity for oxygenated products on Ru–Co/SiO_2 catalysts, which are prepared using Ru–Co bimetallic carbonyl clusters as the metal source, are much higher than those of either Ru or Co monometallic systems. They also found that Ru and Co exist as Ru^0 and Co^{2+}, respectively, and suggested that

bimetallic Ru^0–Co^{2+} sites are very active for the formation of oxygenates in CO hydrogenation (8).

In the field of amine synthesis by nitrile group hydrogenation, both Ru and Co have been known as excellent catalyst metals for producing primary amines with high selectivity and depressing the secondary and tertiary amines compared to other noble metals, such as Rh, Pd, Pt, and Cu (10). However, only a few patents and little literature regarding the synergistic effects of a bimetallic Ru–Co catalyst have been reported on the production of primary amines.

For example, Mashiba disclosed that an unsupported bimetallic Ru–Co catalyst produced 1,4-diaminocyclohexane with high activity and selectivity in the hydrogenation of *p*-phenylenediamine (11). The Berol Chimi A. B. group demonstrated that Ru addition to Co/Al_2O_3 exhibited good selectivity for the desired 1,2-diaminoethane in the amination reaction of monoethanolamine (12).

Nowack *et al.* described that Ru–Co/Al_2O_3, which was prepared from $Co(C_2H_3O_2)_2$ and $K_4[Ru(CN)_5]$, is an effective hydrogenation catalyst for some nitrile compounds, such as acetonitrile and benzonitrile (13).

During our research on developing a nitrile group hydrogenation catalyst, we found that unsupported Ru–Co bimetallic catalysts are very effective in producing primary amines with high activity and selectivity. Especially, these catalysts are very suitable for the reductive amination and CN group hydrogenation of isophoronenitrile to produce isophoronediamine (Scheme I). As the results of the characterization study (we could not get any effective data to realize the structure of these catalysts from X-ray diffraction (XRD), so then we tried temperature programmed reduction (TPR) and X-ray adsorption fine structure (XAFS)), there is a significant interaction between Ru and Co atoms in the case of the catalysts which show high hydrogenation performance.

In this paper, we describe the characterization results of supported and unsupported Ru–Co bimetallic catalysts by the TPR and XAFS, which show clear information of the Ru–Co interaction. We also discuss the hydrogenation results of some nitrile compounds catalyzed by those catalysts.
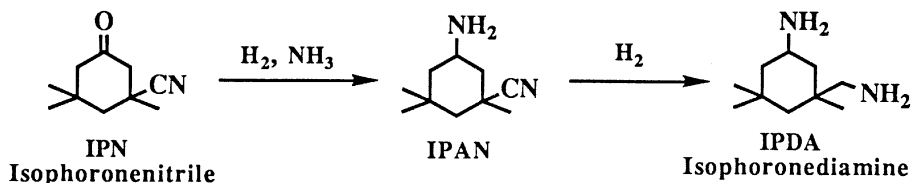
SCHEME I.

EXPERIMENTAL

Catalyst Preparation

Ru and/or Co catalysts supported on SiO_2 were prepared by a conventional technique. SiO_2 (Dokai Chemicals, D-150-300, SA 190 m^2/g) was soaked in an aqueous solution of $RuCl_3 \cdot nH_2O$ (NE Chem Cat) and/or $Co(NO_3)_2 \cdot 6H_2O$ (Kishida Reagents Chemicals). The concentration of the $RuCl_3$–$Co(NO_3)_2$ mixed solution, for example preparing 5% Ru–5% Co/SiO_2, was 11.5 mmol $RuCl_3$–18.3 mmol $Co(NO_3)_2$/100 ml H_2O (excess volume of solution was used). Water was removed by evaporation. Metal precursor-impregnated SiO_2 samples were dried in vacuum at 70°C for 7 h and then allowed to stand for 1 h at rt in contact with 3 N aq NH_3 solution (a little more than the pore volume of SiO_2). These suspensions were filtered, washed with water, and dried under the same conditions stated above. The Ru and Co metal loading was 5 wt% in each case. These dried catalysts (indicating like "5% Ru(OH)x–5% Co(OH)y/SiO_2") could be directly utilized for TPR analysis. These catalysts were reduced at 573 K in flowing H_2 (indicating like "5% Ru–5% Co/SiO_2") before XAFS measurement and hydrogenation reaction.

Ru–Co unsupported catalysts were prepared as follows. An aqueous solution of $RuCl_3$ (34.4 mmol $RuCl_3$/H_2O, 100 ml; pH 1.0) was added dropwise to a Co(OH)x (Wako Pure Chemical Ind.) aqueous suspension (pH 7.4) with vigorous stirring. Added $RuCl_3$ was almost completely adsorbed onto the Co(OH)x, and the supernatant aqueous solution changed to a colorless clear solution. Water of this suspension was removed by evaporation at 363 K, and the residue was treated with 20% NaOH aqueous solution at 373 K (not refluxing) for about 1 h. After cooling, this suspension was filtered, washed with water, and dried in vacuum at 70°C for 9 h, 1, 3, 5, and 10 at.% Ru (as Co atom) loading catalysts were prepared. These dried catalysts (indicating like "5% Ru(OH)x/Co(OH)y") could be utilized for TPR analysis. These catalysts were reduced at 473 K in flowing H_2 (indicating like "5% Ru/Co") before XAFS measurement and hydrogenation reaction.

Temperature Programmed Reduction

The TPR was measured by a continuous-flow method with a thermal conductivity detector. Premixed gas of 5 vol% H_2/Ar (flow rate, 13 ml/min) was passed over about a 25-mg sample in a quartz reactor tube. The temperature was increased from rt to 773 or 1073 K at a constant rate (10 K/min).

X-Ray Absorption Fine Structure

All XAFS spectra at the Co–K edge were measured in the fluorescence mode at RT by a laboratory XAFS spectrometer (Technos EXAC820). An X-ray generator with a rotating Mo anode was operated at 20 kV–210 mA. Johanson-type Ge(220) crystal was used for the monochromator. The detectors for incident and fluorescence X-rays were a sealed proportional counter (sealed Ne gas at 1 atm) and a scintillation counter, respectively. The ratio of fluorescence to scattered incident beam radiation was enhanced using an 8-μm Fe metal foil filter.

XAFS spectra at the Ru–K edge were obtained in the transmission mode on the beam line 10B with a bending magnet at the Photon Factory in the National Laboratory for High Energy Physics. A channel-cut Si(311) was used for the monochromator. The electron storage ring energy was 2.5 GeV, and the ring current was from 300 to 355 mA during experiments. We used two kinds of ion chambers for detectors. One, for monitoring the intensity of an incident beam, was filled with a mixture of 50% Ar and 50% N_2, having 17 cm light-path length. The other, for detecting the intensity of a transmitting beam, was filled with pure Kr gas, with 31 cm light-path length. All XAFS spectra was measured at room temperature.

Ru/Co and Ru–Co/SiO_2 catalyst samples were sealed in air-tight metallic cells which have windows covered with polyimide film in order to avoid oxidization by air. All sampling operation for the XAFS measurement were carried out under dry nitrogen gas atmosphere.

The EXAFS data analysis were performed with the program belonging to a Laboratory EXAFS facility, EXAC820. The EXAFS functions $\chi(k)$ were obtained from the XAFS spectra by subtracting the pre-edge background, followed by cubic spline background removal. The pre-edge background for the Co–K edge data was approximated by a straight line fitted to the pre-edge region, and that for Ru–K edge data was approximated by a Victoreen-type curve, $CE^{-3} + DE^{-4} + \text{constant}$, where E is the photon energy. Normalization was done by dividing by the height of the

TABLE 1

Ranges of the Forward and Inverse Fourier Transform and the Fitting of the First (and the Second) Coordination Shell of Co

Sample	Co–K edge		
	FT range $(k, \text{Å}^{-1})$	FT range $(R, \text{Å})$	CF range $(k, \text{Å}^{-1})$
5% Ru/Co	2.8–11.0	1.55–2.75	4.0–11.0
Co–metal	2.8–11.0	1.55–2.75	4.0–11.0
5% Ru–5% Co/SiO$_2$	2.8–11.0	1.08–2.11	4.0–11.0
5% Ru–5% Co/SiO$_2$	2.8–11.0	2.33–3.18	4.0–11.0
CoO	2.8–11.0	1.10–2.07	4.0–11.0
CoO	2.8–11.0	2.06–3.32	4.0–11.0

absorption edge. The radial structure functions were obtained by Fourier transforms of $k^3\chi(k)$ between 2.8 and 11.0 Å^{-1} for the Co–K edge and between 3.0 and 17.0 Å^{-1} for Ru–K edge data, respectively.

To obtain the structural parameters of the first coordination shell, we performed Fourier filtering and the curve-fitting calculations. The ranges of forward, inverse Fourier transforms and the curve-fitting calculations were given in Table 1 for the Co–K edge data and Table 2 for Ru–K edge data, respectively. The theoretical phase shift and amplitude parameters were cited from the table of McKale *et al.* (14). Since the calculated interatomic distances of Co and Ru metal for the first shell are in good agreement with the crystallographic data, respectively (Co–Co = 2.50 Å, Ru–Ru = 2.67 Å (15)), we consider that the results of these calculations are quite reliable with regard to the interatomic distance for the first shell. We also performed two-shell fitting analyses for the data of the Ru–K-edge of x% Ru/Co catalysts ($x = 3, 5, 10$).

We used the fingerprint method for the XANES spectra analyses in this work. This method is very useful for getting the qualitative information on both geometrical and electronic structures around X-ray absorbing atom.

TABLE 2

Ranges of the Forward and Inverse Fourier Transform and the Fitting of the First Coordination Shell of Ru

Sample	Ru–K edge		
	FT range $(k, \text{Å}^{-1})$	IFT range $(R, \text{Å})$	CF range $(k, \text{Å}^{-1})$
Ru–metal	3.0–17.0	2.00–2.75	4.0–17.0
5% Ru–5% Co/SiO$_2$	3.0–17.0	1.84–2.78	4.0–17.0
5% Ru/Co	3.0–17.0	1.64–2.67	4.0–17.0
3% Ru/Co	3.0–17.0	1.64–2.64	4.0–17.0
10% Ru/Co	3.0–17.0	1.67–2.69	4.0–17.0

Catalytic Hydrogenation and Reductive Amination of Isophoronenitrile

A mixture of 8 g isophoronenitrile (3-cyano-3,5,5-trimethylcyclohexanone), 35 g of methanol, and 15 g of ammonia was introduced into an autoclave (200 ml) and treated at 317 K for 2.5 h in order to convert isophoronenitrile into the corresponding imino compound. After cooling to rt, 1.1 g of 5% Ru/Co catalyst (in the case of 5% Ru–5% Co/SiO$_2$, its weight was 2.7 g), which was reduced in flowing H$_2$ at 473 K (in the case of 5% Ru–5% Co/SiO$_2$, 573 K), was added. These manipulations were performed under Ar atmosphere. Hydrogenation was conducted at 393 K for 1 h, maintaining the total pressure at 7 MPa (or 4 MPa) by continuously inducing hydrogen gas. After the reaction, the reaction mixtures were analyzed by gas chromatography.

Catalytic Hydrogenation of Adiponitrile, Succinonitrile, and Dicyanobenzene

The operations were performed in the same way as described above. In the case of adiponitrile, 100 mmol of adiponitrile, 15 g of methanol, 2.2 g of 5% Ru/Co catalyst (immediately after hydrogen reduction at 473 K), and 15 g of NH$_3$, were placed in an autoclave (200 ml). Hydrogenation was carried out at 393 K for 0.5 h, maintaining the total pressure at 10 MPa by continuously inducing hydrogen gas. After the reaction, the reaction mixtures were analyzed by gas chromatography.

RESULTS AND DISCUSSION

1. Temperature Programmed Reduction

First of all, we studied TPR measurements in order to elucidate the reducibility of the supported and unsupported Ru–Co catalyst precursor. Figure 1 shows the TPR profiles of 5% Ru(OH)x/SiO$_2$ and 5% Ru(OH)x–5% Co(OH)y/SiO$_2$. The TPR spectrum of 5% Ru(OH)x–5% Co(OH)y/SiO$_2$ (Fig. 1b) exhibited only one H$_2$ consumption peak around 443 K, which is quite similar to that of 5% Ru(OH)x/SiO$_2$ (Fig. 1a). This peak at near 443 K was assigned to the reduction of Ru(III) to its metallic state. No other clear peak due to Co(II) reduction was found. Co species supported by SiO$_2$ seem to be less reducible at least under these TPR conditions, even though 5% Ru coexists. (In the case of 5% Ru(OH)x–5% Co(OH)y/SiO$_2$, only a small amount of H$_2$ consumption was observed at over 873 K as a very broad peak; this must be assigned to a part of the Co(II) reduction.)

Contrary to the SiO$_2$ supported catalyst, the reduction of Co compounds, both Co(OH)$_2$ and CoCO$_3$, was observed at 653 and 703 K, respectively (Figs. 2a and 2b). It should be noted that Ru coexisting with Co(II) compounds enhanced the reduction of Co(II) species. The Ru metal plays a role in dramatically dropping the Co reduction temperature from 653 to 543 K (Figs. 2a and 2c) in the case of Co(OH)x and

from 703 to 553 K (Figs. 2b and 2d) for that of $CoCO_3$ (these values are their peak top temperatures in the TPR profiles). These phenomena are thought to be due to spillover hydrogen, which was supplied from metallic Ru to Co(II).

The TPR profiles of Ru(OH)x/Co(OH)y type catalysts with different Ru contents, 1, 5, and 10%, are shown in Fig. 3. A small H_2 consumption peak for the 1% Ru catalyst (Fig. 3a) at 388 K, which is assigned to Ru(III) reduction, shifted to a higher temperature as the loading of Ru increased. On the contrary, the second (508 K) and third (558 K) peak for the 1% Ru catalyst (Fig. 3a), which were assigned to the reduction of Co species, shifted to a lower temperature with increased Ru loading. In summary, as the Ru content increased, the Ru reduction temperature increase and the Co reduction temperature decrease were eventually brought so close together to collapse.

Figure 4b shows the TPR profile of the Ru(OH)x/CoO catalyst. In this catalyst, the main Co(II) reducing peak top temperature was observed at 678 K, which is much higher than those of Ru(OH)x/Co(OH)x and Ru(OH)x/CoCO$_3$. When we prepared this Ru(OH)x/CoO catalyst, it was observed that CoO could not adsorb RuCl$_3$ at all after aqueous RuCl$_3$ solution was added to the CoO–H$_2$O suspension (in the case of Co(OH)x and CoCO$_3$, RuCl$_3$ was completely adsorbed on those Co compounds, and the super-
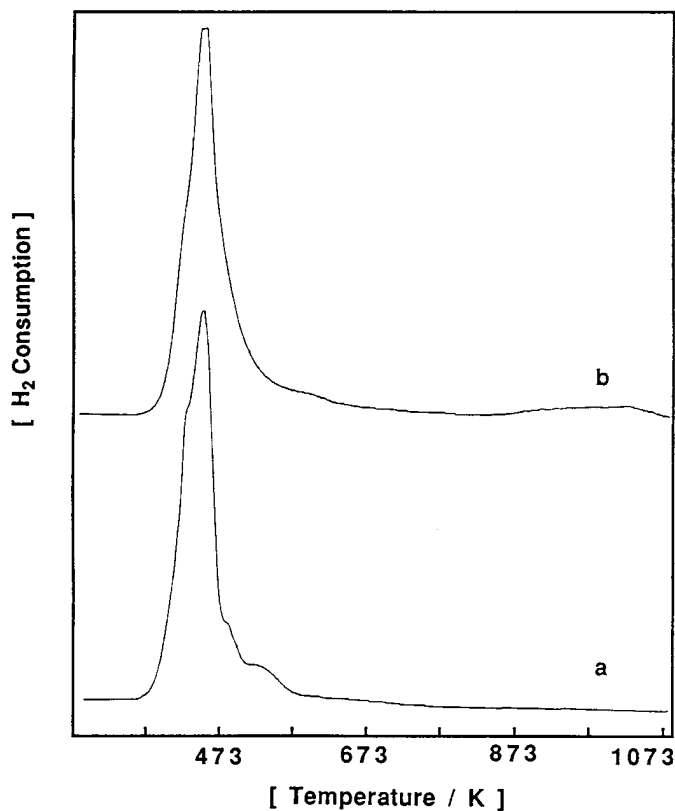

FIG. 2. TPR profiles of unsupported catalysts. (a) Co(OH)x, (b) CoCO$_3$, (c) 5% Ru(OH)x/Co(OH)y, (d) 5% Ru(OH)x/CoCO$_3$.

natant solution became colorless and clear; see Experimental). Ru(OH)x/CoO was then prepared by the evaporation method in order to impregnate RuCl$_3$ on CoO. One of the reasons why the higher Co(II) reduction temperature was required in the Ru(OH)x/CoO catalyst is the weak interaction between RuCl$_3$ and CoO. Accordingly, the Co(II) reduction temperature of Ru(OH)x/CoO was almost the same as that of Co(OH)x alone.

2. X-Ray Adsorption Fine Structure

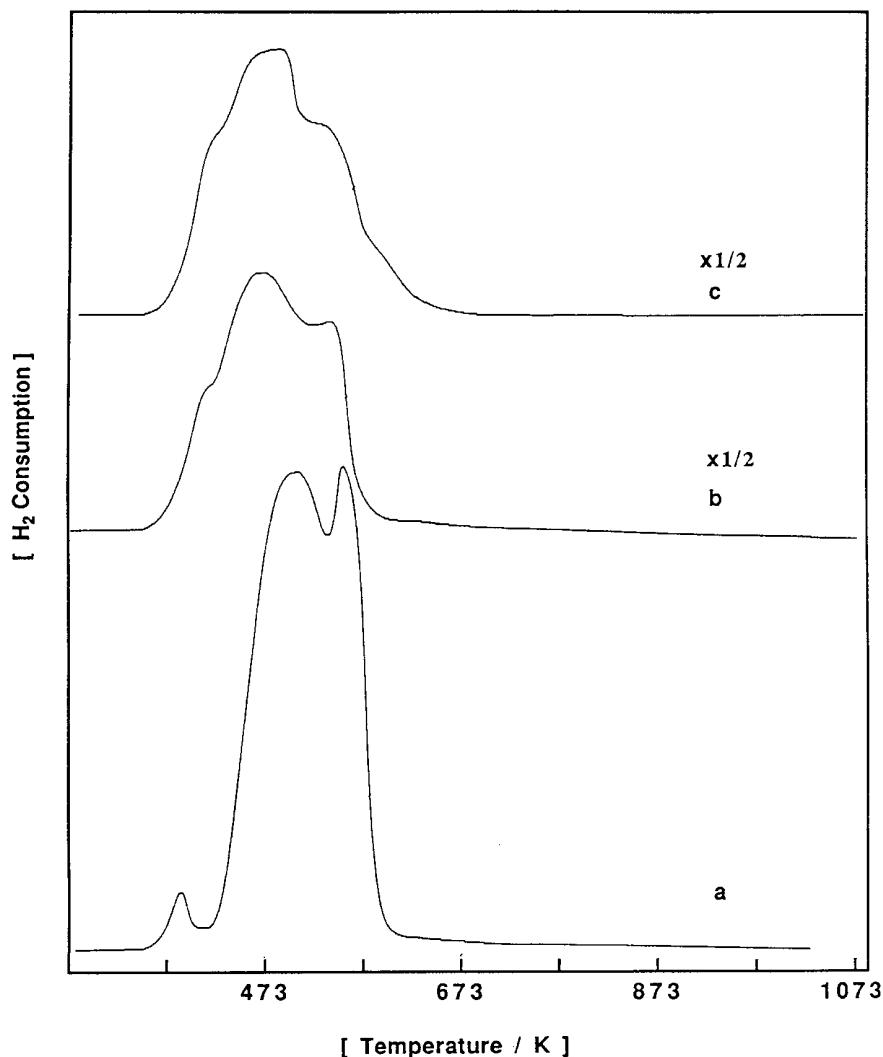The Co–K edge XANES spectra are shown in Fig. 5. The spectrum of 5% Ru/Co catalyst is almost identical to that of

FIG. 1. TPR profiles of SiO$_2$ supported catalysts. (a) 5% Ru(OH)x/SiO$_2$, (b) 5% Ru(OH)x–5% Co(OH)y/SiO$_2$.

FIG. 3. TPR profiles of Ru(OH)x/Co(OH)y; effects of Ru content. (a) 1% Ru, (b) 5% Ru, and (c) 10% Ru.

Co metal. It clearly shows that the Co of 5% Ru/Co catalyst is in metallic state. On the other hand, the spectrum of 5% Ru–5% Co/SiO$_2$ catalyst is similar to that of CoO. It has the strong absorption at the edge and the edge energy shifts toward 12 eV higher than that of Co metal, indicating that the Co of 5% Ru–5% Co/SiO$_2$ catalyst has the character of oxidized Co.

The Ru–K edge XANES spectra are shown in Fig. 6. The profile of the spectra of 5% Ru/Co catalyst is similar to that of Ru metal though there are slight differences between them, and it is quite different from that of RuO$_2$. The edge energy position of the catalyst is almost the same of Ru metal. These results show that the Ru of the catalyst is in the metallic state, but that the local structure around Ru is different from the pure Ru metal.

The extracted EXAFS functions from Co–K edge data are shown in Fig. 7 and from Ru–K edge data are shown in Fig. 8, respectively. Though the Co–K edge EXAFS func-

tion of 5% Ru/Co is very similar to that of Co metal, the Ru–K edge EXAFS function of 5% Ru/Co is slightly different from that of Ru metal.

Figure 9 shows the Fourier transforms of the Co–K edge EXAFS and the calculated interatomic distances are shown in Table 3. In the case of the 5% Ru–5% Co/SiO$_2$ catalyst, two main peaks are observed at 1.5 and 2.8 Å, which could be assigned to the Co–O (2.04 Å) and Co–Co (3.11 Å) contribution by the curve-fitting calculation, implying that most of the Co atoms in the 5% Ru–5% Co/SiO$_2$ catalyst are in the oxidized state. On the contrary, in the case of 5% Ru/Co catalyst, the Fourier transform of the EXAFS function is quite similar to that of Co metal. The Co–Co distance of the 5% Ru/Co catalyst is in good agreement with that of Co metal. It is considered that the Co species in the catalyst exist in a metallic state. These EXAFS results show that Co is presented as Co^0 coincide with the TPR results as we discussed in the previous section. However, any information
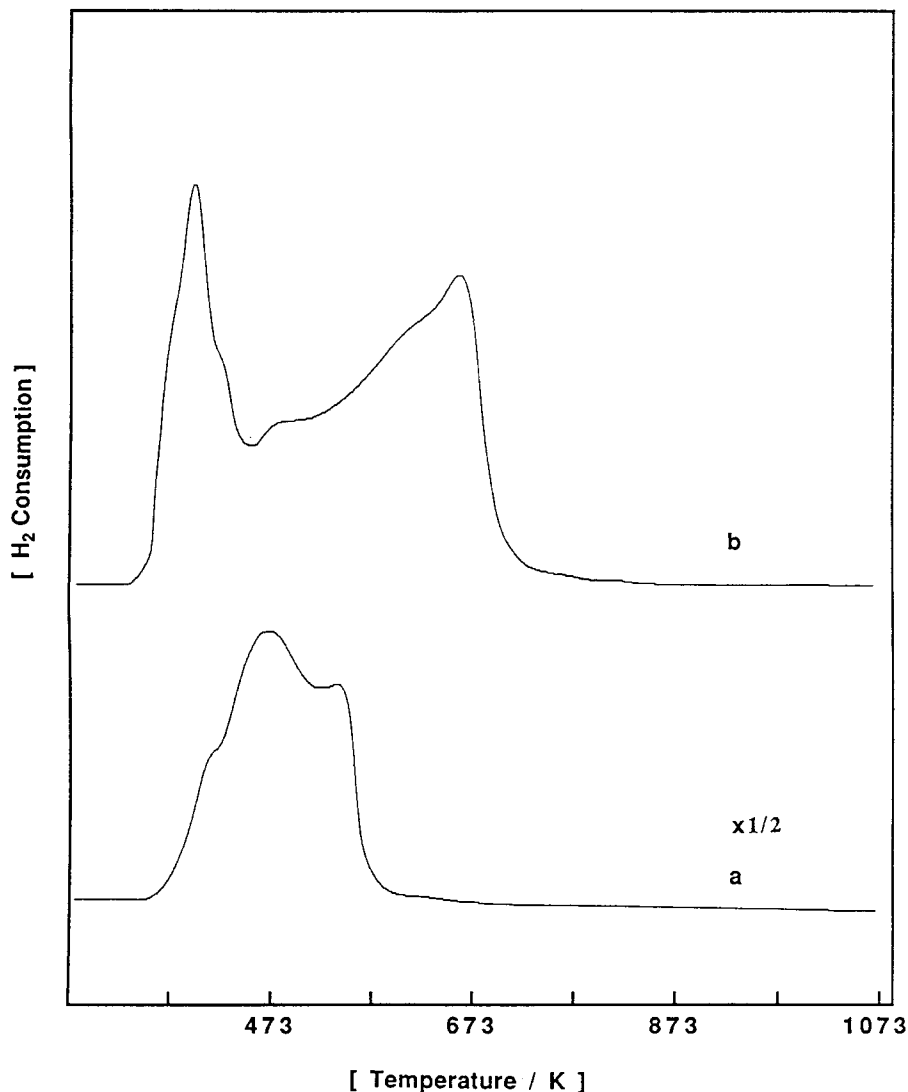
FIG. 4. TPR profiles of (b) 5% Ru(OH)x/CoO. (a) 5% Ru(OH)x/Co(OH)y is used as standard.

on the perturbation of coexisting Ru with Co species in the 5% Ru/Co catalyst could not be obtained from the results of the Co–K edge EXAFS.

The Ru–K edge EXAFS Fourier transforms of Ru metal, the 5% Ru–5% Co/SiO$_2$ catalyst, and the 5% Ru/Co cata-

lyst are shown in Fig. 10 and the calculated interatomic distances of the first shell are listed in Table 4. The first shell of the 5% Ru–5% Co/SiO$_2$ catalyst was assigned to Ru–Ru contribution and the Ru–Ru interatomic distance of 5% Ru–5% Co/SiO$_2$ (2.67 Å) is identical to that of Ru metal foil (2.67 Å). However, the first shell of 5% Ru/Co catalyst

TABLE 3

The Curve Fitting Results of the Interatomic Distances around Co Atoms in Ru/Co, Co–Metal, Ru–Co/SiO$_2$, and CoO

	Co–O (distance, Å)	Co–Co (distance, Å)
5% Ru/Co	—	2.51
Co–metal	—	2.50
5% Ru–5% Co/SiO$_2$	2.04	3.11
CoO	2.08	3.00

TABLE 4

The Curve Fitting Results of the Interatomic Distances around Ru Atoms in Ru–Metal, Ru–Co/SiO$_2$, and Ru/Co

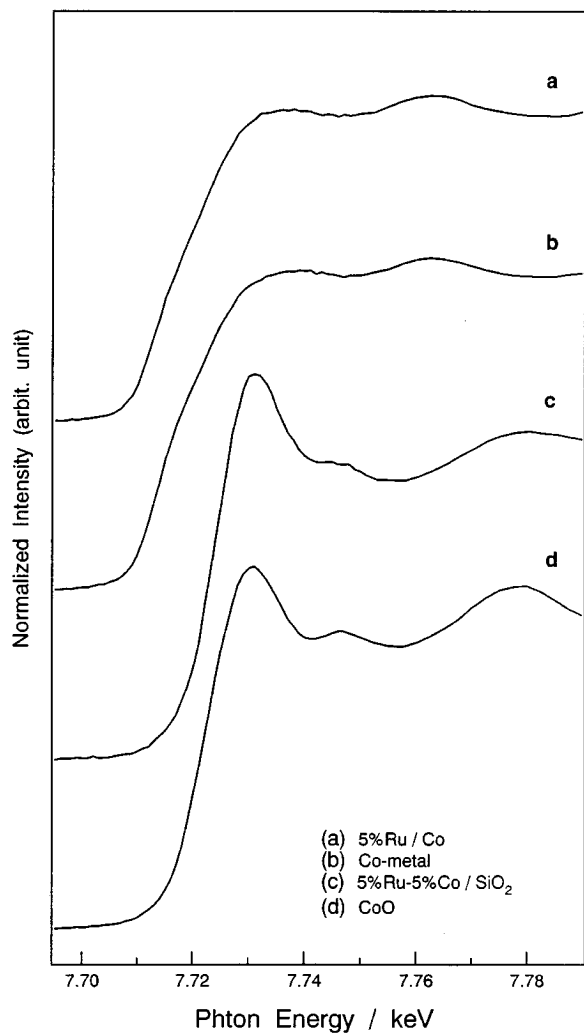|	Atom	Distance Å
Ru–metal	Ru–Ru	2.67
5% Ru–5% Co/SiO$_2$ (in air)	Ru–Ru	2.67
5% Ru/Co	Ru–Co	2.53

FIG. 5. Co–K edge XANES spectra of (a) 5% Ru/Co, (b) Co–metal, (c) 5% Ru–5% Co/SiO$_2$, and (d) CoO.

was not assigned to Ru–Ru but to Ru–Co contribution by the curve-fitting calculation and its interatomic distance is 2.53 Å, which is much shorter than that of Ru metal, but approaching close to the Co–Co bond distance of 2.50 Å in Co metal (Table 3). The important findings in the above results were

(i) Ru is present in a zero valent oxidation state in both the 5% Ru–5% Co/SiO$_2$ and the 5% Ru/Co catalyst,

(ii) Ru in the 5% Ru–5% Co/SiO$_2$ catalyst exists as Ru^0 aggregates,

(iii) Ru in the 5% Ru/Co catalyst does not exist as Ru^0 alone but strongly interacts with Co atoms.

One acceptable understanding of these EXAFS data of the 5% Ru/Co catalyst is the thought that most of the Ru atoms solute into the Co metal crystal framework to form a Ru–Co alloy. Therefore, the observed bond distance in the 5% Ru/Co catalyst is very close to that of Co–Co in

Co metal. E. Iglesa *et al.* reported that the Ru–Co bond distance of the reduced (773 K) 0.14% Ru–11.6% Co/TiO$_2$ is about 2.49–2.52 Å from the Ru–K edge EXAFS results, and these values are smaller than that of the Ru–Ru bond distance in Ru metal (7). Our data are in agreement with their results. On the contrary, in the case of the 5% Ru–5% Co/SiO$_2$ catalyst, Co(II) resists reduction to its metallic state as discussed in the TPR section. Then it is very difficult to form a major amount of Ru–Co alloy on the SiO$_2$ support, and most of the Ru exists without any interaction with Co. As a result, the Ru–Ru distance is observed to be 2.67 Å.

Figure 11 shows the Fourier transforms of the Ru–K edge EXAFS for the three different Ru contents of x% Ru/Co catalysts ($x = 3, 5, 10$). The peak position of the first shell is shifted shorter than that of Ru metal which is the Ru–Ru bond. It is observed that the more the Ru content increases, the broader the peak becomes. In the case of the 10% Ru/Co catalyst, the fitting calculation was not converged by use of
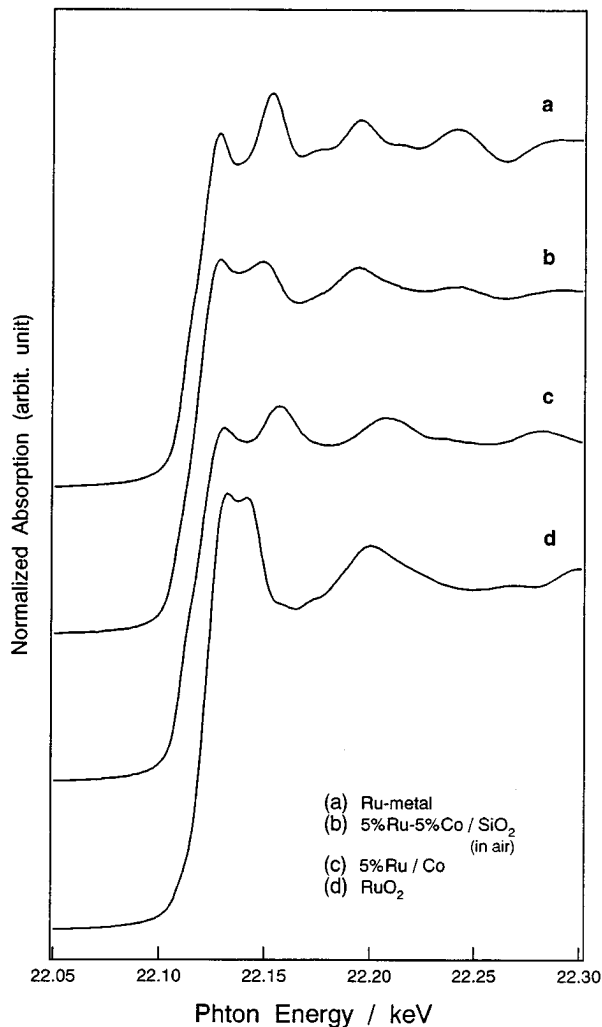

FIG. 6. Ru–K edge XANES spectra of (a) Ru–metal, (b) 5% Ru–5% Co/SiO$_2$, (c) 5% Ru/Co, and (d) RuO$_2$.

only one-shell fitting. These first shells in the Ru/Co catalysts are considered to consist of two contributions, such as Ru–Co and Ru–Ru. We also performed two-shell (Ru–Co, Ru–Ru) curve-fitting analysis for these x% Ru/Co catalysts. The results are shown in Table 5. Since the fitting calculation by use of the tables of McKale is not reliable with regard to the coordination number, we used the ratio of the two coordination numbers; CN(Ru–Co)/CN(Ru–Ru) in the discussion. The ratios are different between the three kinds of catalysts. When we analyzed these data using the ratio CN(Ru–Co)/CN(Ru–Ru), it was found that this ratio increased as the Ru content increased from 3 to 5% but decreased as the Ru content changed from 5 to 10%. These results suggest the following: with increasing Ru content
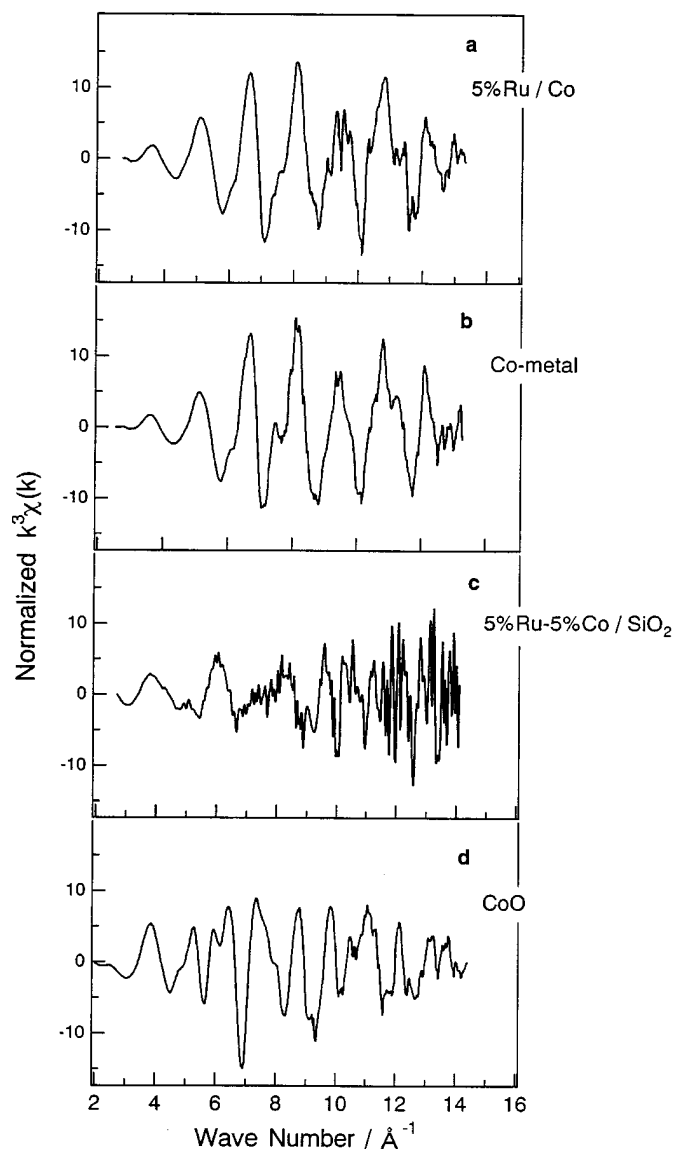

FIG. 7. Co–K edge k^3-weighted EXAFS oscillations of (a) 5% Ru/Co, (b) Co–metal, (c) 5% Ru–5% Co/SiO$_2$, and (d) CoO.
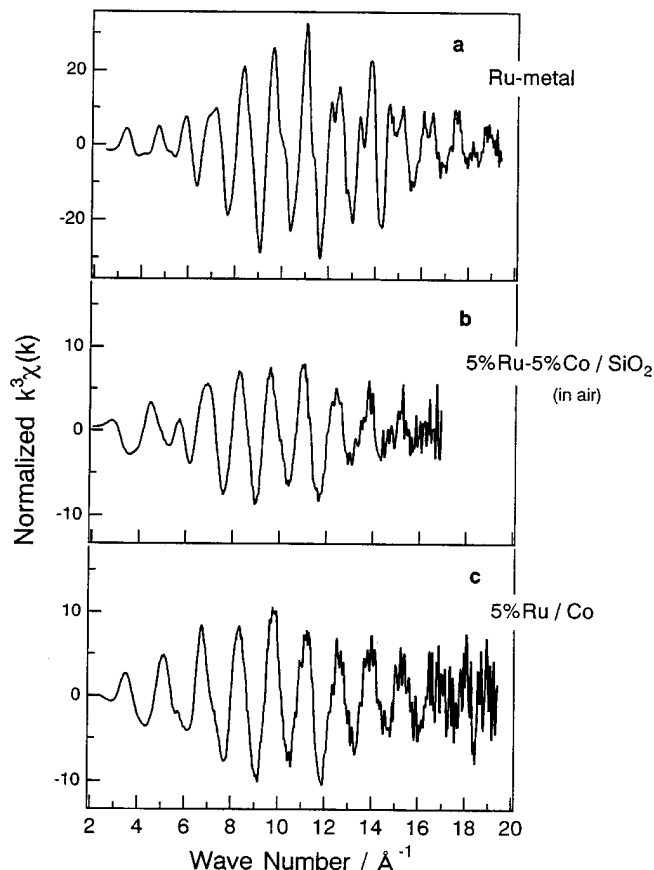

FIG. 8. Ru–K edge k^3-weighted EXAFS oscillations of (a) Ru–metal, (b) 5% Ru–5% Co/SiO$_2$, and (c) 5% Ru/Co.

in this Ru/Co catalyst from 3 to 5%, additional Ru atoms mainly form Ru–Co species to lead the increase of CN(Ru–Co)/CN(Ru–Ru) ratio. However, when the Ru content increases further from 5 to 10%, the additional amount of Ru beyond 5% does not form Ru–Co species any more, but is responsible for forming the Ru–Ru species; then the ratio reversibly decreased.

3. Reductive Amination and Hydrogenation of Isophoronenitrite and Dinitriles

Isophoronenitrile hydrogenation employing several types of Ru–Co bimetallic catalysts was carried out as

TABLE 5

Composition of First Coordination Sphere of Ru Atoms in Ru/Co

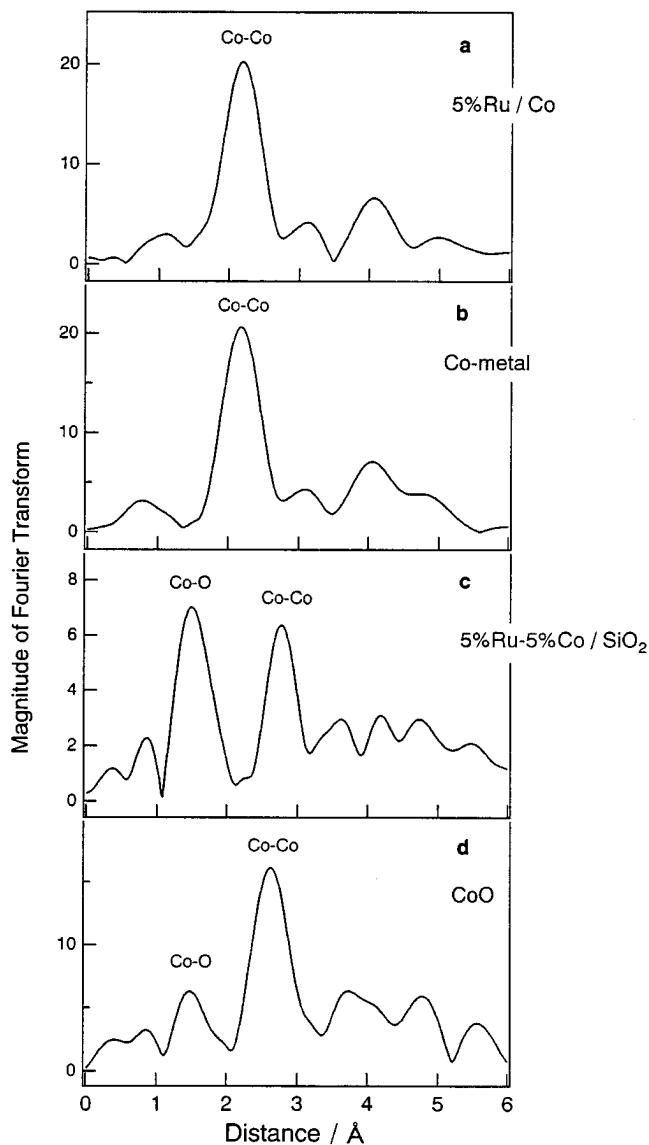|	Distance Å R(Ru–Co) /R(Ru–Ru)	Coordination No. CN(Ru–Co)/CN(Ru–Ru)
10% Ru/Co	2.49/2.66	1.0/1.3
5% Ru/Co	2.52/2.68	1.5/0.2
3% Ru/Co	2.49/2.66	1.9/0.6

FIG. 9. Fourier transforms of Co–K edge k^3-weighted EXAFS oscillations of (a) 5% Ru/Co, (b) Co–metal, (c) 5% Ru–5% Co/SiO$_2$, and (d) CoO.

shown in Table 6. When we used the catalyst, hydrogen-reduced 5% Ru(OH)x–5% Co(OH)y/SiO$_2$, the reaction did not occur under the condition of a total pressure of 7 MPa (H$_2$ was fed continuously). On the contrary, the hydrogen-reduced Ru(OH)x–Co(OH)y ($=$Ru/Co alloy) was found to be a very effective catalyst for this hydrogenation reaction. The hydrogenation activity of this type of catalyst depended on its Ru content; when the Ru content was under 5%, the IPDA productivity increased with increasing Ru content. However, the 10% Ru/Co shows almost the same activity with the 5% Ru/Co.

In order to explain this phenomenon, we proposed the following hypothesis: the catalytic activity must be strongly correlated to the amount of Ru–Co alloy compared to that

of Ru^0 and Co^0 alone. Then, as the Ru content in the catalyst increases from 1 to 5%, additional Ru atoms form mainly Ru–Co species (from EXAFS), and then the catalytic activity increases. However, excessive Ru loading beyond 5% results in the formation of Ru–Ru species (from EXAFS) which do not contribute to improving the catalytic performance for this hydrogenation.

Other interesting results were obtained regarding the Co source. If we used CoO as the Co source to prepare Ru–Co bimetallic catalysts in the same way as the Ru(OH)x/Co(OH)y precursor, this catalyst showed little hydrogenation activity. As we described in the TPR section, RuCl$_3$ was not adsorbed on the CoO when RuCl$_3$ solution was added to the CoO–H$_2$O suspension, and the Co(II) reduction temperature of 5% Ru(OH)x/CoO was higher than that of 5% Ru(OH)x/Co(OH)y or 5% Ru(OH)x/CoCO$_3$. Based on these results, the Ru species of Ru(OH)x/CoO is assumed to interact with the Co species more weakly than that of 5% Ru(OH)x/Co(OH)y or 5% Ru(OH)x/CoCO$_3$, and the Ru–Co hydrogenation active species (alloy) were not formed effectively. It is suggested that this is the reason why Ru(OH)x/CoO has a low hydrogenation activity.
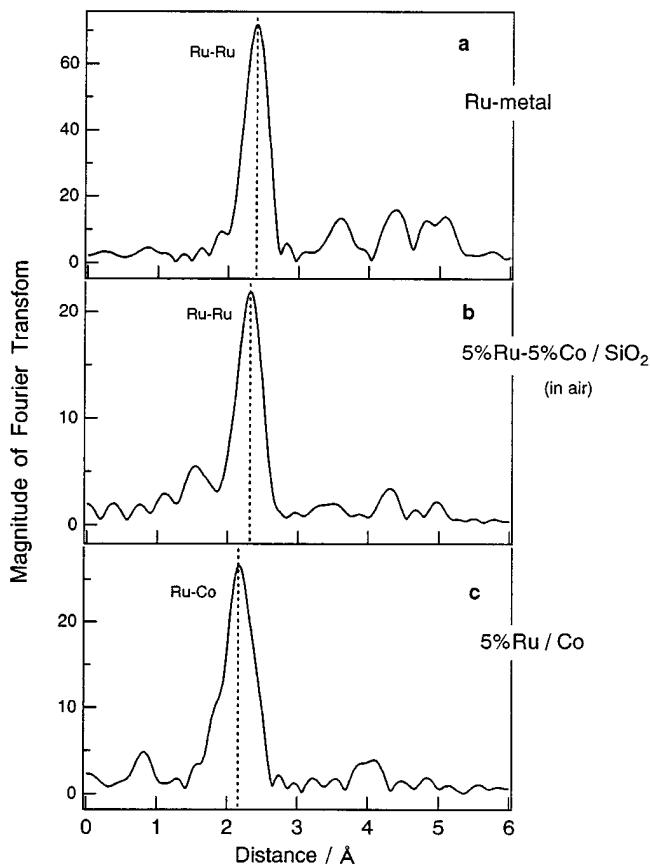

FIG. 10. Fourier transforms of Ru–K edge k^3-weighted EXAFS oscillations of (a) Ru–metal, (b) 5% Ru–5% Co/SiO$_2$, and (c) 5% Ru/Co.

TABLE 6

Reductive Amination and Hydrogenation[a] of Isophorone Nitrile over Several Types of Ru–Co Catalysts

Catalysts (before H$_2$ reduction)	Cat. red. (temp. K)	IPDA Y. (mol%)	IPDA productivity (g IPDA/g cat h)
Co(OH)y	473	NR	—
1% Ru(OH)x/Co(OH)y	473	71.2[b]	5.3
5% Ru(OH)x/Co(OH)y	473	85.5[b]	6.4
10% Ru(OH)x/Co(OH)y	473	83.6[b]	6.2
5% Ru(OH)x–5% Co(OH)y/SiO$_2$	573	NR[c]	—
5% Ru(OH)x/CoO	473	NR	—
5% Ru(OH)x/CoO	623	NR	—
5% Ru(OH)x/Co(OH)y	473	75.4[d,e]	5.6
5% Ru(OH)x/CoCO$_3$	473	85.0[d,f]	6.3[g]

[a] Reaction conditions—Imination: Isophoronenitrile, 48 mmol; MeOH, 35 ml; NH$_3$, 19 eq.; 313 K; 2.5 h. Hydrogenation: H$_2$ pressure, 7 MPa; temperature, 393 K; time, 1 h; cat, 1.1 g.

[b] IPAN remaining amount: 1% Ru; 14.5%, 5% Ru; 7.6%, 10% Ru; 6.9%.

[c] Cat, 2.7 g.

[d] H$_2$ pressure, 4 MPa.

[e] IPAN remaining amount, 11.1%.

[f] IPAN remaining amount, 1.8%.

[g] The best result using this type of catalyst was 6.9 g IPDA/g cat h (The drying method was optimized.) under the same conditions.

Ru(OH)x/CoCO$_3$ also has a high hydrogenation activity, which exceeded the results with Ru(OH)x/Co(OH)y. The reason for this high activity of Ru(OH)x/CoCO$_3$ is not clear but the coexistence of Co(OH)x–CoCO$_3$ (During the preparation of this catalyst, when RuCl$_3$-adsorbed CoCO$_3$ was treated with excess aq. NaOH solution, a part of the CoCO$_3$ must be converted to Co(OH)x. As a result, Co existed as a Co(OH)x–CoCO$_3$ mixture in this catalyst.) functioned in forming the effective species. A similar effect was disclosed by Lok *et al.* in the case of the Ni(OH)$_2$–NiCO$_3$ catalyst (16).

With regard to the Ru(OH)x/Co(OH)y hydrogen reduction temperature, this is a very important factor in its hydrogenation activity, too. Figure 12 shows the relationship of reaction rate vs catalyst H$_2$ reduction temperature. The optimum reduction temperature exists around 473 K, and both higher and lower temperatures resulted in a decrease in hydrogenation activity. The temperature below 473 K must not be enough to reduce Co(OH)x to Co^0; on the other hand, above this temperature Ru–Co alloy sintering probably occurred. If this hypothesis is right, it can be said that the role of Ru, "decreasing the Co reduction temperature," is another essential factor in improving this high hydrogenation activity of the Ru–Co bimetallic catalyst. Indeed, Co(OH)x did not have any hydrogenation activity after 473 K hydrogenation reduction (Table 6), because Co(OH)x itself requires a 100 K higher temperature to be reduced by hydrogen than does Ru(OH)x/Co(OH)y (TPR data).
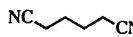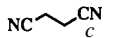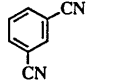
The hydrogenation results of three dinitriles catalyzed by 5% Ru/Co from Ru(OH)x/Co(OH)y are shown in Table 7.

This catalyst reveals a high activity for the hydrogenation of these dinitrile compounds, and their primary amine selectivities are also good or high. Especially adiponitrile was converted to 1,6-hexanediamine in over a 95% yield. We think that this type of Ru–Co bimetallic catalyst has a possibility of becoming a powerful catalyst for producing these industrially important chemicals.

CONCLUSIONS

Both Ru(III) and Co(II) in the unsupported Ru(OH)x/Co(OH)y catalysts were easily reduced to their metallic state completely by H$_2$ reduction at even very low

TABLE 7

Hydrogenation[a] of Dinitriles over Reduced 5% Ru(OH)x/Co(OH)y Catalysts

Dinitriles	Reaction time (h)	Conversion (mol%)	Diamines (yield, mol%)	Diamines productivity (mmol/g cat h)
NC⌒⌒⌒CN	0.5	100	97.2	88
NC⌒⌒CN[c]	2.0	100	62.7[b]	14
(benzene ring with CN, CN)	0.5	100	88.1	80

[a] Reaction conditions: dinitrile, 100 mmol; MeOH, 15 g; catalyst, 2.2 g; NH$_3$, 15 g; H$_2$ pressure, 10 MPa; 393 K.

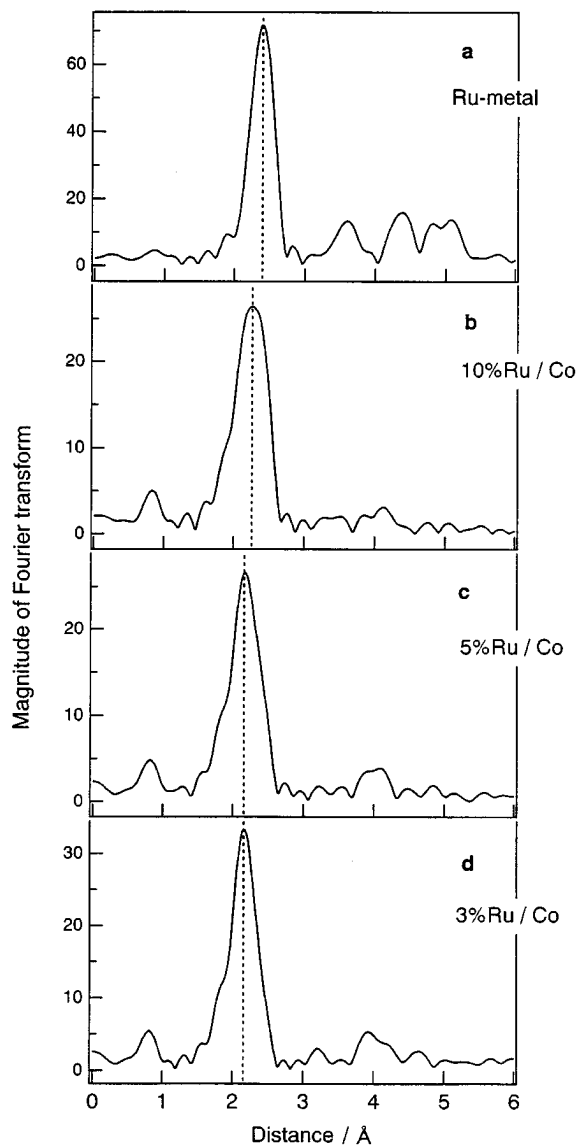[b] Other products: pyrrolidine, 13.6%; aminobutyronitrile, 6.3%.

[c] MeOH, 40 g.

FIG. 11. Fourier transforms of Ru–K edge k^3-weighted EXAFS oscillations of (a) Ru–metal, (b) 10% Ru/Co, (c) 5% Ru/Co, and (d) 3% Ru/Co.

FIG. 12. The effects of 5% Ru(OH)x/Co(OH)y H$_2$ reduction temperature on the hydrogenation activity of isophoronenitrile.

temperatures such as 473 K. XAFS data indicated that Ru and Co were directly bonded; it was suggested that a Ru–Co alloy was formed. On the other hand, the Co(II) of Ru–Co supported on SiO$_2$ catalyst strongly resisted H$_2$ reduction and existed mainly in its oxide state.

The role of Ru in the unsupported Ru–Co catalyst is enhancing the Co(II) reducibility and forming an active species Ru–Co alloy at a very low H$_2$ reduction temperature. As a result, this Ru–Co catalyst has a very effective hydrogenation activity; isophronenitrile was converted to isophronediamine with high activity and selectivity.

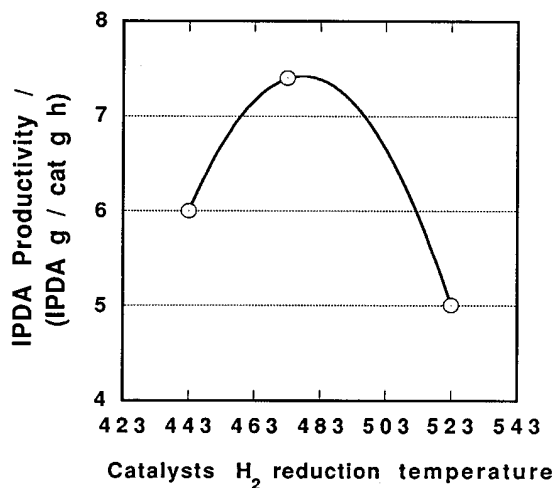The bimetallic catalyst, Ru–Co, was quite effective in the selective hydrogenation of the three dinitrile compounds (adiponitrile, succinonitrile, and dicyanobenzene) to produce corresponding primary diamines at low hydrogen pressure.

REFERENCES

1. Knifton, J. F., and Lin, J.-J., U.S. patent 4,366,259 (1982). [assigned to Texaco, Inc.]
2. Beuther, H., Kobylinski, T. P., Kibby, C. L., and Pannell, R. B., U.S. patent 4,585,798 (1986). [assigned to Gulf Research & Development Co.]
3. Beuther, H., Kibby, C. L., Kobylinski, T. P., and Pannell, R. B., U.S. patent 4,413,064 (1983). [assigned to Gulf Research & Development Co.]
4. Beuther, H., Kibby, C. L., Kobylinski, T. P., and Pannell, R. B., U.S. patent 4,493,905 (1985). [assigned to Gulf Research & Development Co.]
5. Kobylinski, T. P., Kibby, C. L., Pannell, R. B., and Eddy, E. L., U.S. patent 4,605,676 (1986). [assigned to Chevron Research Company.]
6. Kobylinski, T. P., U.S. patent 4,088,671 (1978). [assigned to Gulf Research & Development Co.]
7. Iglesia, E., Soled, S. L., Fiato, R. A., and Via, G. H., *J.Catal.* **143**, 345 (1993).
8. Xiao, F.-S., Fukuoka, A., and Ichikawa, M., *J. Catal.* **138**, 206 (1992).
9. Xiao, F.-S., Fukuoka, A., Ichikawa, M., Henderson, W., and Shriver, D. F., *J. Mol. Catal.* **74**, 379 (1992).
10. Volf, J., and Pasek, J., Hydrogenation of nitriles, *in* "Catalytic Hydrogenation" (L. Cerveny, Ed.), p. 105. 1986.
11. Mashiba, Y., J. patent, 04-18935-A (1992). [assigned to Kawaken Fine Chem.]
12. Kiyoru, Y., J. patent, 05-18627-B (1993). [assigned to Berol Chimi A. B.]
13. Nowack, G. P., Johnson, M. M., and Tabler, D. C., U.S. patent 4,394,298 (1983). [assigned to Phillips Petroleum Comp.]
14. McKale, A. G., Veal, B. W., Paulikas, A. P., Chan, S.-K., and Knapp, G. S., *J. Am. Chem. Soc.* **110**, 3763 (1988).
15. Wyckoff, Ralph, W. G., "Crystal Structures," 2nd ed., Vol. 1, p. 10. 1948.
16. Lok, C. M., and Ritter, H., European patent 496,448 (1992). [assigned to Unichema Chemie BV.]